JOURNAL OF MATERIALS SCIENCE 8 (1973) 1737–1743

The *P–T–x* phase diagram of PbTe and PbSe

B. J. SEALY*, A. J. CROCKER†
Zenith Radio Research Corporation, (UK) Ltd, Stanmore, Middlesex, UK

Pressure–temperature–composition (*P–T–x*) phase diagrams have been calculated for PbTe and PbSe in the temperature range 250°C to the melting point. Various thermodynamic quantities have been estimated which are consistent with electrical parameters measured at room temperature. However, refinements in the band structure and its temperature dependence are needed before an accurate calculation of intrinsic carrier concentration at high temperatures becomes possible.

1. Introduction

The determination of phase diagrams, such as the temperature–composition (or *T–x*) and pressure–temperature (or *P–T*) projections, and the estimation of reaction constants and enthalpies for the lead chalcogenides have been the subject of numerous publications [1-19]. Because of inherent difficulties in vapour-phase equilibration and the long annealing (precipitation) times required at low temperatures, most experimental data exist only for high temperatures. Thus prediction of the equilibrium composition of evaporated thin films deposited onto heated substrates (for $200 \leqslant T \leqslant 400°C$) is not immediately possible. The present work was undertaken in order to predict and control the growth of epitaxial PbTe (PbSe) films and to understand the mechanisms involved in post-growth annealing experiments.

2. Method

In order to calculate *P–T–x* diagrams, various experimental data are required as a function of temperature, (i) the phase width or existence range, (ii) the intrinsic carrier concentration, (iii) the partial pressure of the constituent elements, (iv) the enthalpy of formation and sublimation energy of the compound. The charge state of the predominant defects is also required. Most quantities are available in the literature, although some values are rather uncertain.

2.1. Phase width or *T–x* projection

Annealing and precipitation experiments have been performed and agree with previous determinations of the phase widths of PbTe and PbSe (Figs. 1 and 2) [20]. However, difficulty was experienced with *n*-type PbTe which is clear from the scatter of results in Fig. 1. The straight line portions of the phase extremity in this figure may be represented in terms of the net carrier concentration $| n - p |$ by the equation [21]

$$\mathrm{d}[\ln(n - p)]/\mathrm{d}(1/T) = - \triangle H_{\mathrm{Pb}}/kf \qquad (1)$$

where $\triangle H_{\mathrm{Pb}}$ is the heat involved in reversibly transferring an atom of lead from solid PbTe to the coexistent liquid (Table I). The parameter f is given by

$$f = \left\{\frac{| n - p |/2n_{\mathrm{i}}}{[(| n - p |/2n_{\mathrm{i}})^2 + 1]^{1/2}}\right\} + \left\{\frac{| n - p |/2K_{\mathrm{S}}'^{1/2}}{[(| n - p |/2K_{\mathrm{S}}'^{1/2})^2 + 1]^{1/2}}\right\}$$

where n_{i} is the intrinsic carrier concentration and K_{S}' the ionized Schottky constant. In the region where the compound is in equilibrium with essentially pure Pb (or pure X_2 where $X_2 = Te_2$, Se_2, S_2), the slope may be either $\triangle H_{\mathrm{Pb}}/k$ or $\triangle H_{\mathrm{Pb}}/2k$ depending upon whether $| n - p |$ is

TABLE I Slope of phase width for $T > 400°C$

Slope	PbTe	PbSe
H_{PB}(eV)	0.66	0.50
$H_{\mathrm{X_2}}$(eV)*	0.52	0.30

*$X_2 = Te_2, Se_2$.

*Present address: Department of Physics, University of Surrey, Guildford, Surrey.
†Present address: Department of Physics, Thames Polytechnic, London.

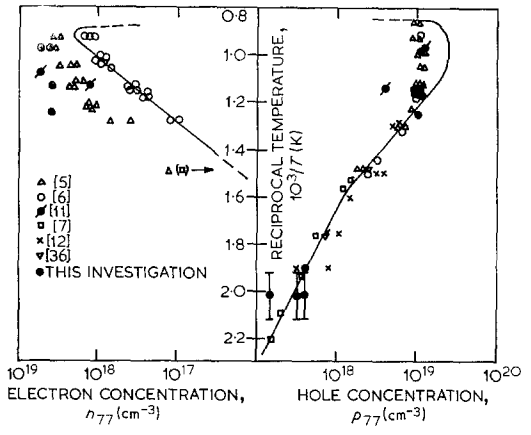

Figure 1 Phase width of PbTe.

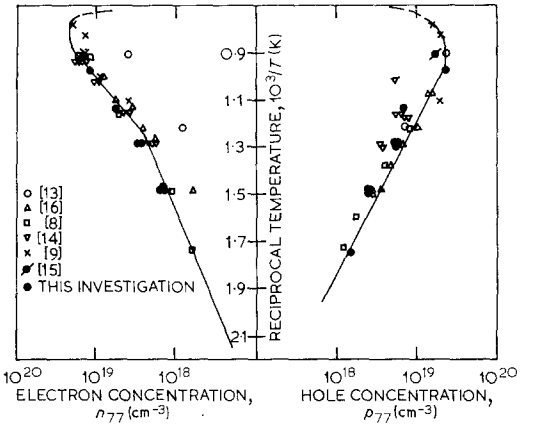

Figure 2 Phase width of PbSe.

intermediate in value between $2n_i$ and $2K_S'^{1/2}$ or large compared with both. This criterion explains the kinks in the locus of the phase extremity for *p*-type PbTe and *n*-type PbSe, (Figs. 1 and 2).

2.2. Intrinsic carrier concentration

The intrinsic carrier concentrations of PbTe and PbSe have been calculated using a two valence band model for the former and a single valance band for the latter, all bands being assumed parabolic. The parameters used in the calculations are shown in Table II. Experimental evidence for a second valence band in PbSe has been obtained [22, 23]. However, assuming a single valence band results in values of n_i 50% greater than experimental ones for PbSe [20]. The presence of two valence bands produces an even greater discrepancy. The values of n_i as a function of temperature for PbSe (Fig. 3) used to calculate the internal structure of the *P–T–x* phase diagram, agree with experiment, and agree with theory only below 300°C. For PbTe there are no available experimental values at high temperatures for a similar comparison to be made.

TABLE II Band parameters used to calculate the *np* product

Parameter	PbS	PbSe	PbTe
E_{g0} (0K), (eV)	0.28	0.14	0.18
E_g (max), (eV)	0.45[a]	0.34[a]	0.35[b]
dE_g/dT[a], (eV K^{-1})	4×10^{-4}	4×10^{-4}	4×10^{-4}
E_v (300K), (eV)	0.38†	0.38†, 0.37‡	0.10[c]
m_{d1}/m_0 (hole) (300K)	0.40[d]	0.35[e]	0.35[f]
m_{d2}^*/m_0 (hole) (300K)	—	0.9‡	2.1[c]
m_e^*/m_0 (electron) (300K)	0.40[d]	0.30[e]	0.25[f]

†Estimated to give reasonable values of n_i at high temperatures.
‡[23].
(a) [37].
(b) Mean of three results, 0.39 eV [37]; 0.34 eV [38]; and 0.33 eV, [39].
(c) [40].
(d) [1]
(e) [39]
(f) [41]

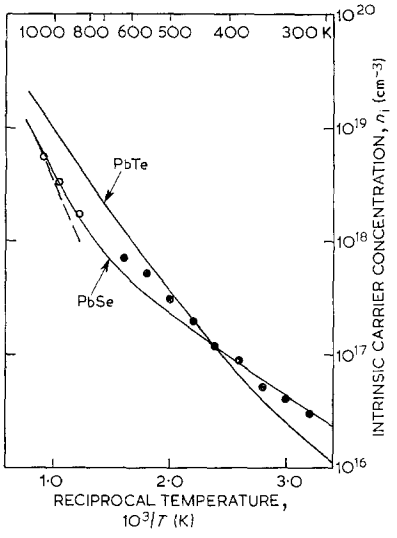

Figure 3 n_i versus $1/T$ for PbTe and PbSe.

2.3. The three phase line

The envelope of the *P–T* diagram is the line along which three phases coexist in equilibrium

and is called the "three phase line". The liquid–vapour–solid and vapour–solid–solid lines are of particular interest here. Part of the three phase line has been determined experimentally for PbTe [17, 18] at high temperatures but at lower temperatures where there are no available data, the three phase line has been represented by the pressure of tellurium (P_{Te_2}) over pure tellurium and the pressure of lead (P_{Pb}) over pure lead [24]. This is a reasonable assumption at low temperatures where PbTe is in equilibrium with essentially pure lead on the lead rich extreme and pure tellurium on the tellurium rich extreme of the existence range. In order to obtain the three phase line at the lead rich extreme of the existence range in terms of P_{Te_2}, Equation A4 was used in conjunction with values of K_{PbTe} after Bis [17] (see Fig. 4).

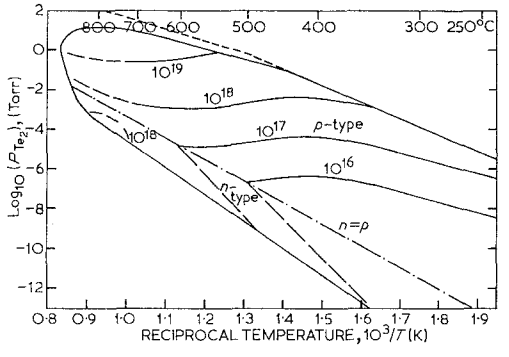

Figure 4 Calculated P–T–x phase diagram for PbTe.

The three phase line for PbSe was obtained from values of K_{PbSe} calculated by Ohashi and Igaki [13] and using published data for the vapour pressure of pure lead and selenium as a function of temperature [24] (see Fig. 5).

2.4. Internal structure of the P–T–x phase diagram

In order to calculate the internal structure of the P–T diagram various points at the phase width (i.e. maximum ionized vacancy or ionized interstitial concentration) were plotted on the three phase line, each point corresponding to a given defect concentration, temperature and partial pressure (P_{Te_2}). From these values and Equations A1, A2 and A4, values of K_{OX} and K_R were calculated using the following electroneutrality conditions:

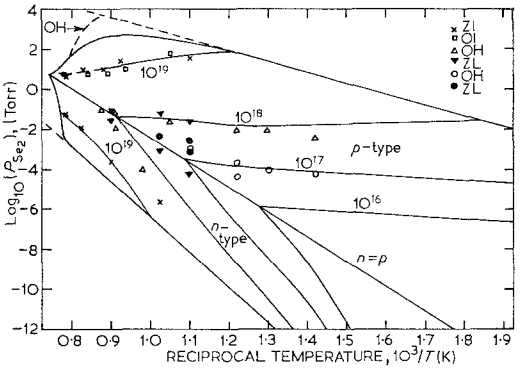

Figure 5 Calculated P–T–x phase diagram for PbSe. Experimental points, ZI [9]; OH, [13].

PbTe (i) $T \gtrsim 700$K, $p = [V_{Pb}']$ p-type
(ii) $T \lesssim 700$K, $p = n_i$ p-type
(iii) All T, $n = n_i$ n-type
PbSe (i) All T, $p = [V_{Pb}']$ p-type
(ii) All T, $n = [Pb_i^{\bullet}]$ n-type

Knowing K_{OX}, K_R and n_i as a function of temperature (Figs. 6 and 7) it was possible to calculate n- and p-type isocarrier concentration lines (Figs. 4 and 5) whose intersection gives values of the ionized Schottky or Frenkel constant (Figs. 6 and 7).

3. Discussion

3.1. Schottky verus Frenkel disorder

Bloem and Kröger [2] assumed Schottky disorder to predominate in PbS at high temperatures but lead interstitials have been deduced as being present in all three lead chalcogenides from tracer diffusion experiments as a function of non-stoichiometry [25-29]. Density and lattice parameter measurements also indicate that lead interstitials and not selenium vacancies are the most abundant defect in lead-rich PbSe [30]. In fact, the diffusion experiments indicate that the defect structure consists of Frenkel defects on the cation sublattice, i.e. lead interstitials, for lead-rich [25-29] and lead vacancies for chalcogen-rich lead chalcogenides [25, 31, 32].

The analysis of Frenkel disorder in a binary compound is identical to the Schottky defect case. Thus, we assume that the n-type conductivity of lead rich material is owing to singly ionized interstitials.

3.2. PbTe

There are very few published experimental results to compare with the present calculations

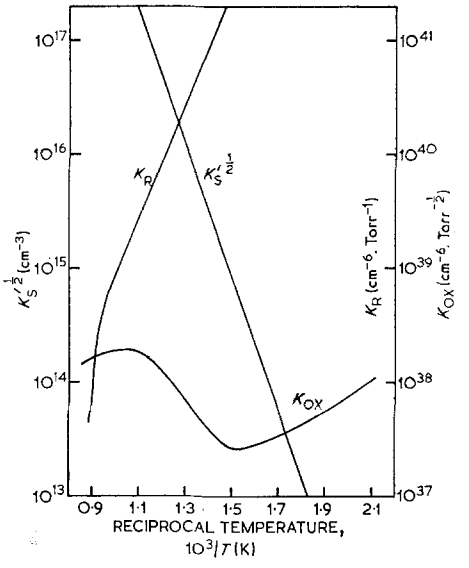

Figure 6 Reaction constants of PbTe as a function of temperature.

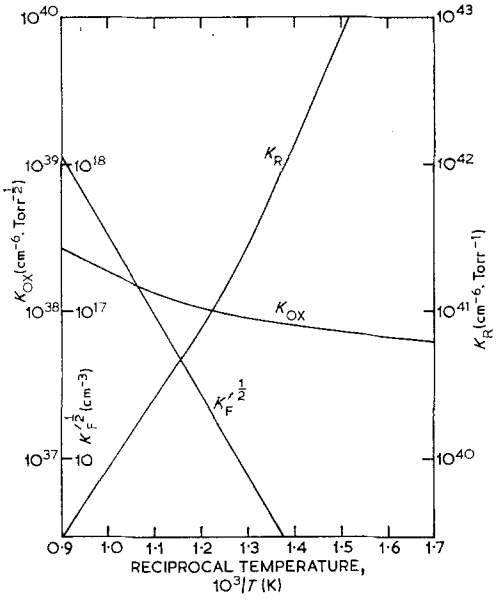

Figure 7 Reaction constants of PbSe as a function of temperature.

of the internal structure of the *P–T–x* phase diagram. Values of K_i from Fujimoto and Sato [11], (FS), are appreciably lower than those calculated here (Fig. 3). However, by re-drawing their diagrams of vacancy concentration versus $K_{OX}P_{Te_2}^{1/2}$ to fit their experimental points, it was possible to show that FS results are consistent with the authors'. Table III compares reaction constants obtained from the adjusted experimental results of FS [11] with those calculated here.

Most reaction constants obtained from FS are less than the authors', but the high temperature results (750°C) agree reasonably well. The differences in the K_i values, if not experimental, can be accommodated by adjusting parameters in the calculations, e.g. effective masses, energy gap, temperature dependences, non-parabolicity of energy bands, variations in scattering mechanisms, values of which are uncertain at elevated temperatures. At 600°C it is difficult to reconcile the differences. However, the FS K_{OX} value is less than the authors' because the formers' carrier concentration is not the equilibrium value at the phase boundary (see Fig. 1), i.e. $[V_{Pb}']$ is too low, presumably because of an insufficiently long annealing time.

3.3. PbSe

Although there are more experimental data available for PbSe than for PbTe, the phase width measurements have not, until now, been related to the internal structure (experimental) of the *P–T–x* diagram. Neither have the results been extrapolated to low temperatures where they should give useful guidance to the preparation of PbSe films. Thus, the PbSe results presented here represent a more detailed analysis over a wider temperature range than do previous

TABLE III Comparison of experimental (FS) [11] and calculated reaction constants for PbTe

Temperature (°C)	Reaction constants					
	K_S (cm^{-3})		K_i (cm^{-6})		K_{OX} (cm^{-6} Torr$^{-\frac{1}{2}}$)	
	FS	T–x	FS	T–x	FS	T–x
750	8.5×10^{17}	8×10^{17}	6×10^{18}	10^{19}	1.3×10^{38}	1.8×10^{38}
600	2.0×10^{17}	10^{17}	2×10^{18}	6×10^{18}	6.4×10^{37}	1.7×10^{38}

investigations.

The calculated internal structure of the P–T diagram compares well with experiment (Fig. 5) although a number of inconsistencies were apparent at high temperatures on the p-side. These were reconciled by adjustment of K_{OX} values so that experimental and calculated internal structure coincided. But this adjustment suggested that the three phase line at high temperatures [13] was incorrect, so a new line was estimated to be consistent with experiment. Although this recalculated line disagrees with the results of Ohashi and Igaki by about an order of magnitude at some points, it is preferred because a departure from ideal behaviour is most likely at these temperatures, i.e. the vapour pressure of selenium over p-type PbSe is probably less than that over pure selenium, suggesting a decrease in activity coefficient to a value less than unity; cf. PbS [2], ZnTe [33], CdTe [33], HgTe [34], PbTe [18] where the activity of Te_2 (S_2) has decreased considerably at high temperatures.

3.4. General discussion

There are a number of points which have not been mentioned so far which warrant some discussion. The first point is that there is a small error present in the position of the lead rich phase boundary of the P–T diagram because no allowance was made for the temperature dependence of the enthalpy of formation of PbTe and PbSe.

The concentration of ionized defects at temperature TK may be written as [1]

$$K_a = 4(2\pi m_0 kT/h^2)^{3/2} (m_{d1}^*/m_0)^{3/2} \exp(-E_a/kT) \quad (3)$$

If we assume the effective mass $m_{d1}^* \propto T^{1/3}$, then Equation 3 becomes

$$K_a \propto T^{5/2} \exp(-E_a/kT) \propto \exp(-E_a'/kT) \quad (4)$$

where E_a and E_a' are the actual and effective ionization energies of the defects. For PbS in the range 1000 to 1200K, Kröger [1] assumed $E_a \sim 0.01$ eV giving $E_a' \sim 0.14$ eV. For the lead chalcogenides there is doubt as to the value of E_a because recent band structure calculations suggest that there is no ionization energy of defects in PbTe [35]. Furthermore, there has been no experimental observation of the freeze-out of carriers at low temperatures ($\sim$ 4.2K). Thus no attempt has been made to calculate values of K_{B_2V} and K_{AV} from the respective K_{OX} and K_R values (see Appendix).

Finally the enthalpies of several reactions for PbTe and PbSe are compared with those for PbS (Table IV), all values being estimated at high temperatures ($\sim$ 800 to 1100K). For PbTe there is agreement with the results of Bis [17].

The PbSe results (Table IV) are numerically less than those calculated by Zlomanov [9], but his data and those of Ohashi and Igaki [13] are consistent with the calculations reported here (see Fig. 5).

TABLE IV Comparison of some reaction enthalpies for the lead chalcogenides ($T \sim$ 800 to 1100K)

Enthalpy (eV)	PbTe	PbSe	PbS*
H_S (or H_F)	2.9†	3.0†	2.5
E_i	0.58	0.78	1.0
H_S' (or H_F')	2.3	2.2	1.78
H_R	−1.0	−0.94	−1.34
H_{OX}	0.53	0.30	0.64

*Results taken from [1], which uses $E_a' = E_b' = 0.14$ eV.
†Calculated assuming $E_a' = E_b' \sim 0$, i.e. $H_S = H_S' + E_i$.

Because of the variations reported in some experimentally determined parameters and the assumptions required for the calculations, the results reported in this paper may need some adjustment as and when new and more reliable data appear. However, it is thought the results will be of help for example, in predicting the electrical properties and the annealing characteristics of epitaxial thin films.

Appendix

Equilibrium between the solid and the gas phase

If a crystal compound AB is in equilibrium with a gas phase the interaction between the solid and gas may be represented by the following equations assuming Schottky disorder predominates [1, 2]

$$A(g) \rightleftharpoons A_A^x + V_B^x + H_{AV}, \quad [V_B^x] = P_A K_{AV} \quad (A1)$$

$$\tfrac{1}{2}B_2(g) \rightleftharpoons B_B^x + V_A^x + H_{B_2V}, \quad [V_A^x] = P_{B_2}^{1/2} K_{B_2V} \quad (A2)$$

where g denotes the gaseous form of A and B, and P the vapour pressure. The notation follows that of Kröger [1]. The enthalpy, H, of a reaction is related to the reaction constant, K, by the equation,

$$K = K^\circ \exp(-H/kT) \quad (A3)$$

where the pre-exponential, K°, can be temperature dependent. The relation between the heat of formation, H_{AB} and the partial pressures of the component species is

$$P_A P_{B_2}{}^{1/2} = K_{AB} = K_S/K_{AV}K_{B_2V} \quad \text{(A4)}$$

K_S being the Schottky constant. The incorporation of atoms from the gas phase can produce charged defects,

$$V_B{}^x \rightleftharpoons V_B{}^\bullet + e' + E_b, \; [V_B{}^\bullet]\, n = K_b \quad \text{(A5)}$$

and

$$V_A{}^x \rightleftharpoons V_A' + h^\bullet + E_a, \; [V_A']\, p = K_a \quad \text{(A6)}$$

E_a and E_b are the ionization energies and n and p are the concentrations of electrons and holes respectively. The combination of Equations A1, A2, A5 and A6 gives

$$A(g) \rightleftharpoons A_A{}^x + V_B{}^\bullet + e' + H_R, \; [V_B{}^\bullet]\, n = P_A K_R \quad \text{(A7)}$$

$$\tfrac{1}{2}B_2(g) \rightleftharpoons B_B{}^x + V_A' + h^\bullet + H_{OX}, \; [V_A']p = P_{B_2}{}^{1/2}K_{OX} \quad \text{(A8)}$$

where writing $K_R = K_A + K_b$ and $K_{OX} = K_B V + K_a$ is often more convenient. Using the mass action equation for the np product (Equation A9) we may obtain further relationships, e.g.

$$0 \rightleftharpoons e' + h^\bullet + E_i, \quad np = K_i \quad \text{(A9)}$$

$$K_S' = K_S K_a K_b / K_i \quad \text{(A10)}$$

and

$$H_S' = H_S + E_a + E_b - E_i \quad \text{(A11)}$$

the primes (Equations A10 and A11) referring to the ionized Schottky constant (enthalpy). Electroneutrality (Equation A12) and the equality of the number of A and B sublattice sites imposed by the crystal structure (Equation A13) represent other important conditions:

$$n + [V_A'] = p + [V_B{}^\bullet] \quad \text{(A12)}$$

$$[A_A{}^x] + [V_A{}^x] + [V_A'] = [B_B{}^x] + [V_B{}^x] + [V_B{}^\bullet]. \quad \text{(A13)}$$

At high temperatures the dominant neutrality conditions $n = [V_S{}^\bullet]$ and $p = [V_{Pb}']$ apply to PbS for lead- and sulphur-rich material, respectively [2]. On substitution into the above equations we obtain:

$$n^2 = \frac{K_S K_b}{P_{S_2}{}^{1/2} K_{S_2V}} \quad \text{(A14)}$$

$$p^2 = K_{OX} P_{S_2}{}^{1/2} \quad \text{(A15)}$$

$$n^2 = K_R P_{Pb}. \quad \text{(A16)}$$

The introduction of Frenkel disorder of the cation sublattice does not affect the calculations but different nomenclature is required to distinguish Frenkel from Schottky disorder. If the electroneutrality condition for n-type PbSe is $n = [Pb_i{}^\bullet]$ then Equation A7 will become:

$$A(g) \rightleftharpoons A_A{}^x + A_i{}^\bullet + e' + H_{Ri}, \quad [A_i{}^\bullet]\, n = P_A K_{Ri} \quad \text{(A7a)}$$

the values of K_R and K_{Ri} being identical.

Acknowledgements

The authors wish to acknowledge the help and advice of Dr Mino Green and Dr L. M. Rogers.

References

1. F. A. KRÖGER, "The Chemistry of Imperfect Crystals" (North Holland, Amsterdam, 1964).
2. J. BLOEM and F. A. KRÖGER, *Z. Phys. Chem.* **7** (1956) 1.
3. J. R. STUBBLES and C. E. BIRCHENALL, *Trans. Met. Soc. AIME* **215** (1959) 535.
4. A. J. STRAUSS, *ibid* **239** (1967) 794.
5. R. F. BREBRICK and R. S. ALLGAIER, *J. Chem. Phys.* **32** (1960) 1826.
6. R. F. BREBRICK and E. GUBNER, *ibid* **36** (1962) 1283.
7. W. W. SCANLON, *Phys. Rev.* **126** (1962) 509.
8. H. ABRAMS, Ph.D. Dissertation, Lehigh University, USA (1968).
9. V. P. ZLOMANOV, O. V. MATVEEV and A. V. NOVOSELOVA, *Vestnik Moskov Univ.* **5** (1967) 81; **6** (1968) 67.
10. K. IGAKI and N. OHASHI, *Bull. Univ. Osaka Prefecture* **11** (1962) 89.
11. M. FUJIMOTO and Y. SATO, *Jap. J. Appl. Phys.* **5** (1966) 128.
12. T. L. KOVAL'CHIC and IU. P. MASLAKOVETS, *Sov. Phys. Tech. Phys.* **1** (1956) 2337.
13. N. OHASHI and K. IGAKI, *Trans. Jap. Inst. Met.* **5** (1964) 94.
14. R. F. BREBRICK and E. GUBNER, *J. Chem. Phys.* **36** (1962) 170.
15. A. V. NOVOSELOVA, V. P. ZLOMANOV and O. V. MATVEEV, *Inorg. Mat.* **3** (1967) 1154.
16. A. R. CALAWA, T. C. HARMAN, M. FINN and P. YOUTZ, *Trans. Met. Soc. AIME* **242** (1968) 374.
17. R. F. BIS, Naval Ordnance Lab. Tech Report, 61-128 (1961); *J. Phys. Chem. Solids* **24** (1963) 579.
18. R. F. BREBRICK and A. J. STRAUSS, *J. Chem. Phys.* **40** (1964) 3230.
19. F. C. ABBOTT, Ph.D. Thesis, University of Delaware (1965).
20. B. J. SEALY, Ph.D. Thesis, University of Surrey (1972).
21. R. F. BREBRICK, *J. Appl. Phys. Suppl.* **33** (1962) 422.
22. M. N. VINOGRADOVA, I. M. RUDNIK, L. M. SYSOEVA and N. V. KOLOMOETS, *Sov. Phys. Semicond.* **2** (1969) 892.
23. M. N. VINOGRADOVA, *ibid* **3** (1969) 231.
24. R. E. HONIG and D. A. KRAMER, *R.C.A. Rev.* **30** (1969) 285.

25. M. P. GOMEZ, D. A. STEVENSON and R. A. HUGGINS, *J. Phys. Chem. Solids* **32** (1971) 335.
26. T. D. GEORGE and J. B. WAGNER, *J. Appl. Phys.* **42** (1971) 220.
27. M. S. SELTZER and J. B. WAGNER, *J. Chem. Phys.* **36** (1962) 130; *J. Phys. Chem. Solids* **24** (1963) 1525.
28. G. SIMKOVICH and J. B. WAGNER, *J. Chem. Phys.* **38** (1963) 1368.
29. K. R. ZANIO and J. B. WAGNER, *J. Appl. Phys.* **39** (1968) 5686.
30. H. GOBRECHT and A. RICHTER, *J. Phys. Chem. Solids* **26** (1965) 1889.
31. M. S. SELTZER and J. B. WAGNER, *ibid* **26** (1965) 233.
32. Y. BAN and J. B. WAGNER, *J. Appl. Phys.* **41** (1970) 2818.
33. A. S. JORDAN and R. R. ZUPP, *J. Electrochem. Soc.* **116** (1969) 1285.
34. R. F. BREBRICK and A. J. STRAUSS, *J. Phys. Chem. Colloids* **25** (1964) 1441.
35. N. J. PARADA and G. W. PRATT, *Phys. Rev. Letters* **22** (1969) 180.
36. T. D. GEORGE and J. B. WAGNER, *J. Phys. Chem. Solids* **30** (1969) 2359.
37. A. F. GIBSON, *Proc. Phys. Soc.* **65** (1952) 378.
38. R. N. TAUBER, A. A. MACHONIS and I. B. CADOFF, *J. Appl. Phys.* **37** (1966) 4855.
39. L. M. ROGERS and A. J. CROCKER, to be published.
40. L. M. ROGERS, *Brit. J. Appl. Phys.* **18** (1967) 1227.
41. G. W. JOHNSON, *J. J. Electron Control* **12** (1962) 421.

Received 24 May and accepted 22 June 1973.